Quadruple-Responsive Nanocomposite Based on Dextran–PMAA–PNIPAM, Iron Oxide Nanoparticles, and Gold Nanorods

Wenqian Feng, Weipeng Lv, Junjie Qi, Guoliang Zhang, Fengbao Zhang, Xiaobin Fan*

A quadruple-responsive nanocomposite that responds to temperature, pH, magnetic field, and NIR is obtained by incorporating superparamagnetic iron oxide nanoparticles (SPIONs) and gold nanorods (AuNRs) into a dextran-based smart copolymer network. The dual-sensitive copolymer is prepared by sequential RAFT polymerization of methacrylic acid and *N*-isopropylacrylamide from trithiocarbonate groups linked to dextran in one pot. These functionalized nanocomposites with superior stability can respond to the four stimuli mentioned above well. As evidenced by UV–vis and TEM measurements, the temperature-induced unusual blue-shift in the longitudinal plasmon band is possibly due to the side-to-side assembly of AuNRs.

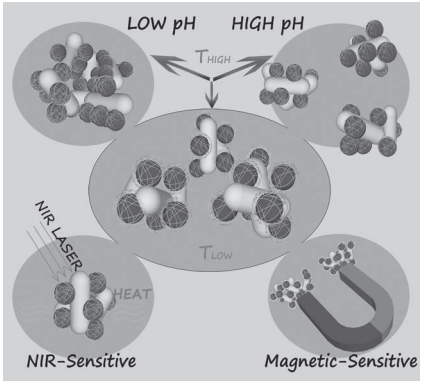

1. Introduction

Stimuli-responsive nanomaterials, also referred as smart nanomaterials, have attracted considerable research interest due to the capability of dynamically changing their physical and chemical properties upon exposure to external stimuli.[1,2] Various smart materials have been designed and pursued for practical applications, such as biomedical imaging, biological detection, and drug delivery.[3–7] Among them, poly(*N*-isopropylacrylamide) (PNIPAM) is one of the most widely studied temperature-responsive polymers, which is soluble in water below lower critical solution temperature (LCST) but undergoes a sharp phase transition to aggregate state above LCST.[8] Pure PNIPAM has a readily accessible LCST ≈32 °C, which can be further adjusted in a wide range by incorporating new components into the PNIPAM chains.[9] In particular, the incorporation of polymers containing ionizable weak acidic or basic moieties can not only adjust the LCST of PNIPAM, but also generate copolymers that can additionally respond to pH.[10–12] Near infrared radiation (NIR) is an important stimulus for photo-induced therapeutic applications because of its deep penetration and low absorption in tissues.[13] When PNIPAM-based polymers are conjugated with nanomaterials with strong absorption in NIR region, such as gold nanorod (AuNR), the heat generated by photothermal effect will elevate the local environmental temperatures and result in a phase transition of PNIPAM-based polymers, which in turn induces the variation of intrinsic properties of conjugated nanomaterials.[11,12,14,15] Moreover, magnetic nanoparticles that respond to magnetic field also hold another promising stimulus for biological applications as they can be used for diagnostic imaging and detection by magnetic resonance imaging (MRI), as well as for building targeted delivery vehicles.[16] Despite the encouraging progress in smart nanomaterials, many of them are still unexplored, and novel smart nanomaterials responding to multiple stimuli (temperature, pH, magnetic field, and NIR) at the same time are desirable for modern diagnostic and therapeutic applications.

W. Feng, Dr. W. Lv, Dr. J. Qi, Prof. G. Zhang, Prof. F. Zhang, Dr. X. Fan
School of Chemical Engineering and Technology, Tianjin University, Tianjin 300072, P. R. China
E-mail: xiaobinfan@tju.edu.cn

Macromol. Rapid Commun. **2012**, *33*, 133–139

DOI: 10.1002/marc.201100595

Early in our work, we have previously functionalized and endowed gold nanoparticles with stability and stimuli sensitivity using a series of dextran-based smart polymer.[17–19] These polymers are synthesized by reversible addition–fragmentation chain transfer (RAFT) polymerization using 2-(dodecylthiocarbonothioylthio)-2-methylpropanoic acid (DTM) esterificated dextran (DEX–DTM) as macrochain transfer agent (CTA) and NIPAM as "smart" monomer. Herein, we report the rational design and facile preparation of a novel robust and quadruple-responsive nanocomposite (QNC) that can respond to temperature, pH, magnetic field, and NIR at the same time. With the assistance of a dextran-based temperature- and pH-responsive copolymer dextran-b-poly[methacrylic acid (MAA)]-b-poly(*N*-isopropylacrylamide) (DEX–PMAA–PNIPAM), superparamagnetic iron oxide nanoparticles (SPIONs), and AuNRs were sequentially incorporated into the copolymer network, resulting in these QNCs.

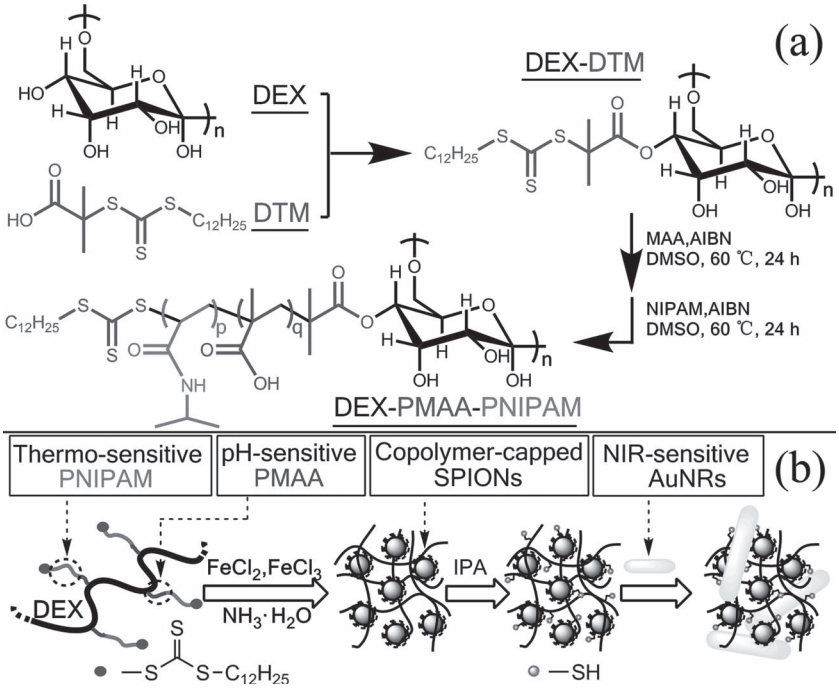

Scheme 1. (a) Scheme of synthesis of DEX–PMAA–PNIPAM copolymer by RAFT polymerization in one-pot. (b) Coprecipitation of SPIONs using dextran-based copolymer as nucleating and stabilizing agent and subsequent attachment of AuNRs through Au–S bonds.

2. Experimental Section

2.1. Materials

Dextran ($\overline{M}_W$ = 70 000, Seebio Biotechnology) was used as received. *N*-Isopropylacrylamide (NIPAM, 97%, Aldrich), and 2,2′-azobisi-sobutyronitrile (AIBN, 98%, Aldrich) were recrystallized twice from hexane and methanol, respectively. Methacrylic acid (MAA, 99%, Aldrich) was distilled before used. The macrochain transfer agent DEX-DTM was synthesized according to the literature. All other reagents were purchased from commercial sources and used as received.

2.2. One-Pot Synthesis of DEX–PMAA–PNIPAM by RAFT Polymerization

Ten milliliters of DMSO solution containing DEX–DTM (0.24 g, ≈50 μmol), MAA (14.2 μL, 167 μmol), and AIBN (1.55 mg, 9.42 μmol) was added in a 100 mL round-bottomed flask and degassed by purging with N_2 for 30 min and then placed in a water bath thermostat at 60 °C. After 24 h, NIPAM (0.355 g, 3.137 mmol) and additional AIBN (2.5 mg) were added. The reaction was allowed to proceed at 60 °C for another 24 h. At last, the copolymer was purified by dialysis against water for 3 d using a 14 000 molecular weight cut-off (MWCO) dialysis tube (regenerated cellulose, Spectra/Por4) and recovered after lyophilization.

2.3. Synthesis of QNCs

Gold nanorods with controlled aspect ratio were synthesized by using the seed-mediated growth method.[20] To remove the excess hexadecyltrimethylammonium bromide (CTAB), the as-prepared AuNRs solution were purified twice by centrifugation at 17 300 g for 15 min and redispersed in the same volume deionized water (18 mΩ) while the supernatant was removed.

Superparamagnetic iron oxide nanoparticles were synthesized by coprecipitation.[21] A mixture of $FeCl_3$•$6H_2O$ (46.6 mg, 0.172 mmol) and the copolymer (100 mg, ≈12 μmol) in 10 ml degassed deionized water (18 mΩ) was placed in a 100 mL three-neck flask equipped with a strong stirring device. The solution was chilled to 4 °C while bubbling with nitrogen for 30 min. A freshly prepared solution of $FeCl_2$•$4H_2O$ (20 mg, 0.100 mmol) was added to the flask using a syringe. Immediately, NH_3•H_2O (25%, 1 mL) was added to the mixture with rapid stirring and then heated. The reaction vessel was kept at 60 °C for 2 h under nitrogen. The SPIONs solution was purified by dialysis against water for 3 d using a 14 000 MWCO dialysis tube and the solid sample was obtained by lyophilization.

Isopropylamine (10.7 mg, 180 μmol, 15-fold molar excess vs. thiocarbonylthio groups) was added in SPIONs embedded in copolymer suspensions (10 mg mL^{-1}), and the reaction was carried out for 2 h in ice-cold water bath. Then, the solution pH was adjusted to neutral by adding 0.1 M HCl solution. Then CTAB–free AuNRs and SPIONs solutions with various volume ratios were mixed and stirred for 2 h. All procedures performed under a nitrogen atmosphere. The resulting solution was centrifuged at 8 800 g to remove unbound SPIONs. The solid sample was obtained by lyophilization.

3. Characterization

^{1}H NMR spectra were obtained on a Bruker DRX-500 spectrometer operating at 400 MHz. FTIR measurements were carried out on a Nicolet Nexus FTIR Spectrometer using KBr pellets. Transmission electron microscopy (TEM) images were collected by using a Philips Tecnai G2F20 high-resolution transmission electron microscope. ζ-potential measurements were carried out with a Malvern nano ZS using highly dilute dispersions. UV–vis spectra were recorded using a Unico 2802 spectrometer. Dynamic light scattering (DLS) measurements were carried out using Brookhaven Instruments BI-200SM goniometer equipped with a BI-9000AT correlator at a 532 nm wavelength and a detection angle of 90°. The magnetization measurements of dried samples were carried out at room temperature using a vibrating sample magnetometer (VSM, LDJ9600-1) with a maximum applied field of 10 kOe. In the photothermally induced temperature-rising measurement, 20 mg dried QNCs dispersed in 10 mL PBS buffer at pH 7.4 were irradiated at 750 nm (1.5 W power), and the temperature of the dispersion was monitored with a thermocouple probe placed inside the cuvette.

4. Results and Discussion

The smart copolymer DEX–PMAA–PNIPAM was prepared by sequential RAFT polymerization of MAA and NIPAM using DEX–DTM as macro-CTA and AIBN as radical initiator in one pot; see Scheme 1a. This dextran-based macro-CTA was synthesized by esterification of dextran (= 70 000) with a versatile chain transfer agent DTM, which can offer many unique opportunities to: (1) (co) polymerize many kinds of monomers in a facile and controlled RAFT polymerization; (2) provide biocompatibility, biodegradability, and resistant coatings for nanomaterials with the aid of hyperbranched dextran,[22] and (3) by aminolysis, the polymer with trithiocarbonate groups can be converted into thiol terminated and subsequently immobilized on the gold surface through stable Au–S bonds.[17,23] According to the previous reports,[24] when the molar ratio of MAA increases, LCSTs of the copolymers shift to higher temperature and disappear when the mole ration of MAA is higher than 7.5%. Hence, 5.0 mol% MAA based on the total mol of the monomers were used in the polymerization. The copolymers were identified by FTIR spectra (Figure S1, Supporting Information), and the peaks at 1644, 1546, and 1712 cm^{-1} are attributed to the –C=O, –NH and –COOH groups, respectively, suggesting the successful addition of NIPAM and MAA to the DEX–DTM chains. The compositions of copolymer were determined by using ^{1}H NMR spectra (Figure S2 and S3, Supporting Information).[25] Approximately, 13–14 DTM groups are linked to one dextran chain (= 70 000), and 3–4 MAA, and 65–67 NIPAM units are grafted to one DTM chain. This result confirms that the versatile dextran-based CTA can be successfully used for sequential RAFT polymerization of a series of monomers. As depicted in Scheme 1b, the copolymer is composed of hydrophilic backbones (dextran) and modified side chain (PNIPAM-b-PMAA).

SPIONs for in vivo use are usually produced by coprecipitation from an alkaline solution containing iron salts as precursor and dextran as the coating polymer.[21,26,27] By using our dextran-based smart copolymer as nucleating and stabilizing agent, SPIONs were successfully prepared and incorporated into a smart network. The narrow size distribution (10 ± 3.5 nm) determined by TEM image (Figure 1a) benefits from: (1) the existence of dextran as

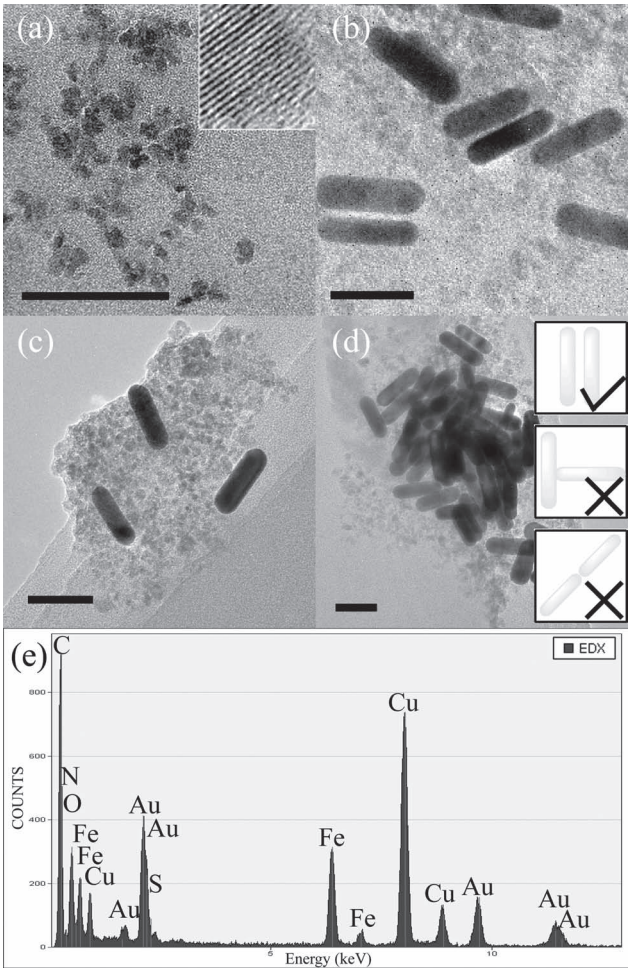

Figure 1. TEM images of (a) SPIONs; (b) and (c) dispersed QNCs, AuNRs, and SPIONs are incorporated in the copolymer network; (d) randomly aggregated state of QNCs at 50 °C pH 4.5, side-to-side arrangements are dominant; (e) EDX spectrum of QNCs corresponding to (c); (scale bars: 50 nm). Inset: Schematic of AuNRs assembles in side-to-side, end-to-side, and end-to-end orientations.

surface coating material; (2) the strong covalent interaction between carboxylate groups of MAA and surface iron cations; (3) and multiple anchor points in every copolymer chain. Notably, the aqueous hydrodynamic radius (R_h) of SPIONs observed by DLS falls in 66–69 nm (Figure S4, Supporting Information), which is much larger than the particle size observed by TEM, confirming the existence of the long-chain copolymer network around the SPIONs.

After converting the copolymers surrounding SPIONs into thiol terminated by aminolysis, CTAB–free AuNRs (57 × 16 nm) were mixed with SPIONs solutions with various volume ratios and subsequently attached to the copolymer covalently through Au–S bonds. By using this strategy, SPIONs and AuNRs were sequentially incorporated into the copolymer network, resulting in the quadruple-responsive QNCs; see Scheme 1b. The unbound SPIONs were separated by centrifugation. As demonstrated by the TEM images (Figure 1b and c) and the EDX spectrum (Figure 1e, corresponding to Figure 1c), SPIONs, AuNRs, and copolymer strongly interacted with each other, as indicated by the close assemble of SPIONs around AuNRs and the coexistence of Au, Fe, N, O, and S signals. Previously, we found that gold nanoparticles that were functionalized by dextran-based smart polymers were stable under various harsh conditions.[17,18] Likewise, both of the SPIONs and nanocomposites aqueous solutions were also found to be stable even in concentrated salt (1 M) solution for 1 week and no sedimentation was observed.

As PNIPAM block in the side chain of copolymer undergoes a reversible conformational transition from hydrophilic to hydrophobic state when heated above LCST,[9] the aggregation states and optical properties of the QNCs are temperature tunable. The influence of temperature on the optical properties of the QNCs was studied by UV–Vis spectroscopy in the temperature range from 25 to 50 °C at pH 4.5 (Figure 2a). When the temperature increases above 29 °C, the absorbance increases steadily (from 0.95 to 1.50). Interestingly, an obvious blue-shift of the maximum wavelength (λ_{max}) in the longitudinal plasmon band was observed (from 734 to 719 nm) as well. Previous studies on AuNR–PNIPAM systems revealed that temperature-induced red-shift, in contrast to blue-shift, was a general phenomenon due to the changes of (1) the local refractive index near the gold surfaces, and/or (2) the plasmon coupling, depending on the aggregation states of the AuNRs.[13–15] In the former case, the increase of local refractive index induced by the collapse of PNIPAM will result in the increase of the absorbance and λ_{max} frequency, and the degree of increase is related to the density of PNIPAM surrounding AuNRs. For the latter one, when interparticle distances of AuNRs are short enough, the plasmon coupling occurs because of electronic interactions.[28] Given the interactions can be

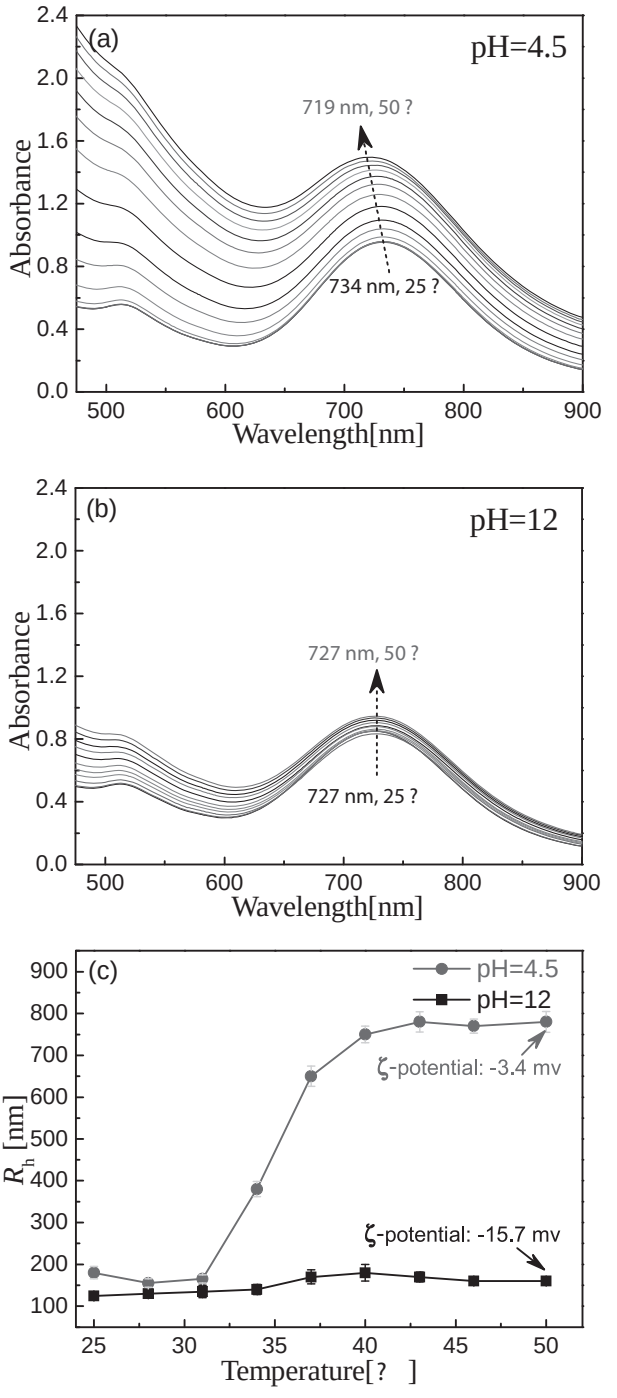

Figure 2. UV–Vis absorption spectra of the QNCs at (a) pH 4.5 and (b) pH 12 at different temperatures; (c) R_h of the QNCs versus temperature at pH 4.5 and 12. At pH 4.5, an obvious blue-shift of λ_{max} (15 nm) can be observed; the decrease and increase of R_h at 29 and 33 °C indicate the collapse of copolymer and the aggregation of QNCs, respectively. At pH 12, the thermosensitivity is much weakened. The difference of λ_{max} at 25 °C between pH 4.5 and pH 12 may be attributed to the slight side-to-side assembly of Au NRs in alkaline solution, which is in good agreement with previous reports.[22,29] The LCST is defined as the temperature that the absorbance at 600 nm starts to increase.

classified into end-to-end, end-to-side and side-to-side, different assembly states of the anisotropic AuNRs may have opposite effects on the λ_{max}. In Karg's system,[12,14] AuNRs were decorated on the surface of PNIPAM-based microgels due to electrostatic attraction, in which, end-to-end and end-to-side interactions of AuNRs were dominant and an obvious red-shift occurred when the microgel shrank. In Rodriguez–Fernandez's system,[15] the AuNRs were encapsulated in PNIPAM shells, which were so thick that the close contact of AuNRs was hampered, resulting in weak electronic interactions among AuNRs. The increase and red-shift of the absorption peak was mainly due to the increase of refractive index, not aggregation of AuNRs. However, the copolymer network in our system is arranged in a loosely compact hairy form around AuNRs rather than the dense microgel or thick shell. When the QNCs were randomly aggregated into large agglomerate without spatial restriction, side-to-side arrangements of AuNRs, as evidenced by TEM images (Figure 1d), were dominant. Therefore, the blue-shift of λ_{max} in our system can be explained by the balance of two opposite effects: (1) "decreased" aspect ratio due to side-to-side arrangement, hence blue-shifted λ_{max}; and (2) increased local refractive index, which cause the red-shift of the λ_{max} and yet should be ignored due to the low density of the PNIPAM. Figure S6 (Supporting Information) shows that the aggregation of these QNCs is completely reversible over 6 cycles, revealing the robust nature offered by the copolymer coating.

Next, we investigate the pH-sensitivity of the nanocomposites, that is, distinctive temperature-dependent optical properties at different pH values. The significant difference between the blue-shift of λ_{max} in pH 4.5 (15 nm) (Figure 2a) and in pH 12 (0 nm) (Figure 2b) indicate the arrangements of AuNRs are intensely affected by pH above LCST, which is in good agreement with previous reports.[10–12] The pH-sensitivity can be attributed to the charge density of the QNCs at different pH, as revealed by ζ-potential measurements. At pH 4.5 (lower than the pK_a 6–7 of PMAA), PMAA is protonated (ζ-potential = −3.4 mV), and the LCST phase transition of PNIPAM results in the increase of interparticle hydrophobic interaction, the aggregation of AuNRs, and a significant blue-shift step by step. However, upon ionization at higher pH value (ζ-potential increases from −3.4 to −15.7 mV at pH 12), increasing electrostatic repulsion prevents the QNCs from large-scale aggregation, displaying as no blue-shift. Moreover, with the increase of temperature to 50 °C, R_h increase to 780 and 150 nm at pH 4.5 and 12, respectively (Figure 2c). This is different from the microgel in Karg's system.[12] When heated above LCST, the collapse of PNIPAM chain induced a decrease in spherical volumes of microgel and a plasmon coupling of the decorated AuNRs even in relatively high pHs. In our system, without the cross-linker agent, the copolymer surrounds the metal nanoparticles loosely. The different R_h values of QNCs at various temperatures and pH confirm the formation of large aggregates at lower pH and the prevention of close contact of AuNRs by electrostatic repulsion at higher pH. Hence, no blue-shift of the λ_{max} can be observed in high pHs. Not only does the intermolecular repulsion weaken the blue-shift but also it limits the increase of absorbance by prohibiting copolymers from interchain self-association. In addition, pH also has significant effects on LCST, which is 29 °C at pH 4.5 and 35 °C at pH 12, because the changes in the hydrophobicity of PMAA affect the hydrophilic/hydrophobic balance of the copolymers.[10]

The magnetic properties of SPIONs and QNCs were examined via vibrating sample magnetometer (VSM) measurements (Figure 3a). Neither of them shows remanence or coercivity, indicating they have superparamagnetic property at room temperature. Figure 3b–e illustrates the separation of SPIONs and QNCs in the presence

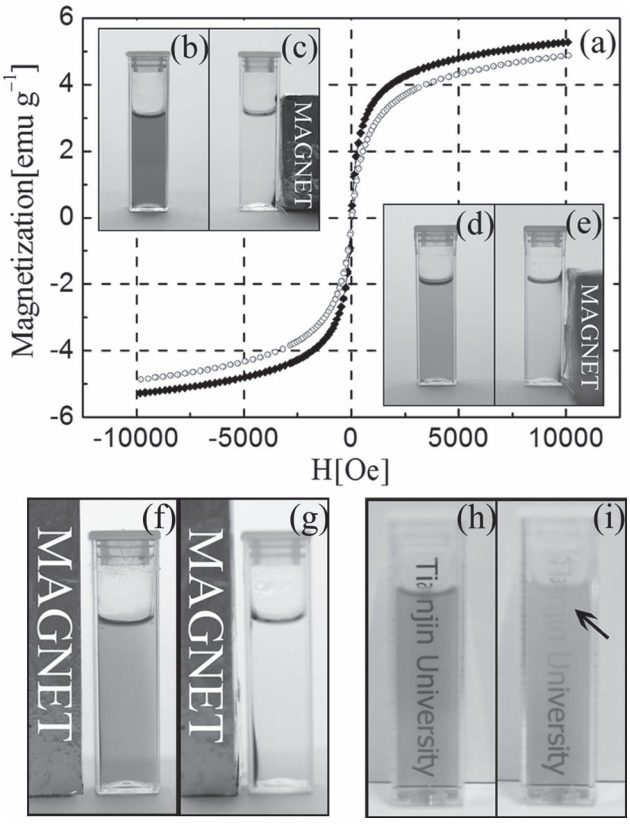

Figure 3. (a) Magnetization curve of SPIONs (♦) and the nanocomposites (○) at room temperature; Photographs of SPIONs neutral solutions before (b) and after (c) as well as the QNCs neutral solutions before (d) and after (e) application of a magnet (≈500 mT) at 25 °C for 48 h; Photographs of QNCs neutral solution under the influence of a magnetic field (≈300 mT) at (f) 25 °C and (g) 50 °C for 4 h; Photographs of the QNCs solution at pH 4.5 (h) before NIR exposition and (i) irradiated at a spot (indicated by arrow) within 2 min.

of a magnetic field within 48 h. For the pure SPIONs with small dimension (10 ± 3.5 nm), they practically remained stable in a magnetic field of 300 mT in a short time because of the slow response to the magnetic field at room temperature (Figure 3f). However, at temperature above LCST (i.e., 50 °C), magnetic separation can be achieved within 4 h (Figure 3g). The enhancement of magnetic interaction is ascribed to the phase-transition induced aggregation of QNCs that causes the rapid response and fast migration under an external magnetic field.[30] Moreover, since the phase transition of the QNCs is reversible, the QNCs could regain excellent water solubility when the temperature decreases below LCST and the magnetic field is removed.

By taking advantage of the NIR-absorption ability of AuNRs, photo-induced variations in optical properties of QNCs were obtained. When exposed to a continuous laser with a wavelength at 750 nm (laser power of 1.5 w), the temperature of the medium solution was increasing gradually (Figure S7, Supporting Information). As the photothermal conversion takes place in the irradiation area, a rapid temperature rising around the laser spot can lead to a phase transition of the surrounding copolymer. The solution (pH 4.5) turned from transparent (Figure 3h) to turbid (Figure 3i) within 2 min when irradiated by NIR laser, and returned to its original state as laser was turned off. Therefore, the fast and addressable phase transition of the copolymer can be reversibly switched on/off by turning on/off the NIR laser irradiation externally. However, for solution at pH 12, it did not exhibit an obvious visual change when applied for the same irradiation (data not shown), which was in line with the results of the UV–Vis absorption spectra (Figure 2a and b).

5. Conclusion

We have successfully prepared a novel quadruple-responsive nanocomposite with superior stability. A dextran-based copolymer exhibiting temperature and pH sensitivities have been used for the in situ formation of SPIONs and incorporating AuNRs in the polymer network. The QNCs could respond to the temperature, pH, magnetic field, and NIR illumination simultaneously. Interestingly, the optical study of the hybrid materials reveals that the aggregation of QNCs will induce an obvious blue-shift in the longitudinal plasmon band of the incorporated AuNRs, possibly due to a side-to-side electronic interaction of the nanorods in this system. As a multifunctional smart nanomaterial, we can envision that these QNCs may possess many practical applications, such as temperature and pH-controlled magnetic separation, temperature-programmed MRI, simultaneous targeting, biolabeling, imaging, photothermal therapy, and magnetic hyperthermia.

Supporting Information

Supporting Information is available from the Wiley Online Library or from the author.

Acknowledgements: This work was supported in part by the Research Fund of the National Natural Science Foundation of China (No. 21106099), the Tianjin Natural Science Foundation (No.11JCYBJC01700) and the Program of Introducing Talents of Discipline to Universities (China, No: B06006).

Received: September 8, 2011; Revised: October 11, 2011; Published online: November 21, 2011; DOI: 10.1002/marc.201100595

Keywords: blue-shift; gold nanorod; reversible addition fragmentation chain transfer (RAFT); stimuli-sensitive polymers; superparamagnetic iron oxide

[1] M. A. C. Stuart, W. T. S. Huck, J. Genzer, M. Muller, C. Ober, M. Stamm, G. B. Sukhorukov, I. Szleifer, V. V. Tsukruk, M. Urban, F. Winnik, S. Zauscher, I. Luzinov, S. Minko, *Nat. Mater.* **2010**, *9*, 101.
[2] Y. Lu, J. Liu, *Acc. Chem. Res.* **2007**, *40*, 315.
[3] C. Wang, J. Chen, T. Talavage, J. Irudayaraj, *Angew. Chem. Int. Ed.* **2009**, *48*, 2759.
[4] H. W. Gu, K. M. Xu, C. J. Xu, B. Xu, *Chem. Commun.* **2006**, 941.
[5] M. S. Yavuz, Y. Y. Cheng, J. Y. Chen, C. M. Cobley, Q. Zhang, M. Rycenga, J. W. Xie, C. Kim, K. H. Song, A. G. Schwartz, L. H. V. Wang, Y. N. Xia, *Nat. Mater.* **2009**, *8*, 935.
[6] Q. S. Wei, J. Ji, J. C. Shen, *Macromol. Rapid. Comm.* **2008**, *29*, 645.
[7] W. J. Kim, I. K. Park, K. Singha, R. B. Arote, Y. J. Choi, C. S. Cho, *Macromol. Rapid. Comm.* **2010**, *31*, 1122.
[8] M. H. Stenzel, *Chem. Commun.* **2008**, 30, 3486.
[9] C. d. l. H. Alarcon, S. Pennadam, C. Alexander, *Chem. Soc. Rev.* **2005**, *34*, 276.
[10] X. Yin, A. S. Hoffman, P. S. Stayton, *Biomacromolecules* **2006**, *7*, 1381.
[11] M. Das, N. Sanson, D. Fava, E. Kumacheva, *Langmuir* **2006**, *23*, 196.
[12] M. Karg, Y. Lu, E. Carbo-Argibay, I. Pastoriza-Santos, J. Perez-Juste, L. M. Liz-Marzan, T. Hellweg, *Langmuir* **2009**, *25*, 3163.
[13] T. Kawano, Y. Niidome, T. Mori, Y. Katayama, T. Niidome, *Bioconjugate Chem.* **2009**, *20*, 209.
[14] M. Karg, I. Pastoriza-Santos, J. Perez-Juste, T. Hellweg, L. M. Liz-Marzan, *Small* **2007**, *3*, 1222.
[15] J. Rodriguez-Fernandez, M. Fedoruk, C. Hrelescu, A. A. Lutich, J. Feldmann, *Nanotechnology* **2011**, *22*, 245708.
[16] A. H. Lu, E. L. Salabas, F. Schuth, *Angew. Chem. Int. Ed.* **2007**, *46*, 1222.
[17] W. P. Lv, S. Q. Liu, X. B. Fan, S. L. Wang, G. L. Zhang, F. B. Zhang, *Macromol. Rapid Comm.* **2010**, *31*, 454.
[18] W. P. Lv, Y. Wang, W. Q. Feng, J. J. Qi, G. L. Zhang, F. B. Zhang, X. B. Fan, *J. Mater. Chem.* **2011**, *21*, 6173.
[19] W. Lv, S. Liu, W. Feng, J. Qi, G. Zhang, F. Zhang, X. Fan, *Macromol. Rapid Comm.* **2011**, *32*, 1101.
[20] B. Nikoobakht, M. A. El-Sayed, *Chem. Mater.* **2003**, *15*, 1957.
[21] B. R. Jarrett, M. Frendo, J. Vogan, A. Y. Louie, *Nanotechnology* **2007**, *18*, 035603.

[22] A. P. Goodwin, S. M. Tabakman, K. Welsher, S. P. Sherlock, G. Prencipe, H. J. Dai, *J. Am. Chem. Soc.* **2009**, *131*, 289.
[23] N. Morinloto, X. P. Qiu, F. M. Winnik, K. Akiyoshi, *Macromolecules* **2008**, *41*, 5985.
[24] C. L. Lo, K. M. Lin, G. H. Hsiue, *J. Control Release* **2005**, *104*, 477.
[25] H. F. Xu, F. H. Meng, Z. Y. Zhong, *J. Mater. Chem.* **2009**, *19*, 4183.
[26] C. Tassa, S. Y. Shaw, R. Weissleder, *Acc. Chem. Res.* **2011**, *44*, 842.
[27] R. Hernandez, C. Mijangos, *Macromol. Rapid Comm.* **2009**, *30*, 176.
[28] M. Gluodenis, C. A. Foss, *J. Phys. Chem. B* **2002**, *106*, 9484.
[29] Z. Sun, W. Ni, Z. Yang, X. Kou, L. Li, J. Wang, *Small* **2008**, *4*, 1287.
[30] J. Qin, Y. S. Jo, M. Muhammed, *Angew. Chem. Int. Ed.* **2009**, *48*, 7845.